Carbohydrate Polymers 237 (2020) 116174

Contents lists available at ScienceDirect

Carbohydrate Polymers

journal homepage: www.elsevier.com/locate/carbpol

In vitro degradability and bioactivity of oxidized bacterial cellulose-hydroxyapatite composites

Erika Patricia Chagas Gomes Luz[a], Paulo Hiago Silva Chaves[b], Lidia de Araújo Pinto Vieira[b], Sádwa Fernandes Ribeiro[b], Maria de Fátima Borges[b], Fabia Karine Andrade[a,b], Celli Rodrigues Muniz[b], Antonia Infantes-Molina[c], Enrique Rodríguez-Castellón[c], Morsyleide de Freitas Rosa[b], Rodrigo Silveira Vieira[a,*]

[a] Federal University of Ceará (UFC), Department of Chemical Engineering, Bloco 709, 60455-760, Fortaleza, Ceará, Brazil
[b] Embrapa Agroindústria Tropical – CNPAT, Rua Dra Sara Mesquita 2270, Pici, 60511-110, Fortaleza, Ceará, Brazil
[c] Department of Inorganic Chemistry, Crystallography and Mineralogy, Faculty of Sciences, University of Malaga, Campus Teatinos s/n, 29071 Malaga, Spain

ARTICLE INFO

Chemical compounds studied in this article:
Sodium periodate (PubChem CID: 23667635)
Hydroxylamine hydrochloride (PubChem CID: 443297)
Ethylene glycol (PubChem CID: 174)
Calcium chloride (PubChem CID: 5284359)
Sodium hydrogen phosphate (PubChem CID: 24203)
Hydroxyapatite (PubChem CID: 14781)
D-glucopyranose (PubChem CID: 5793)
Glycolic acid (PubChem CID: 757)
Hydroxybutyric acid (PubChem CID: 441)

Keywords:
Oxidized bacterial cellulose
Hydroxyapatite
Hybrids composites
Bone tissue

ABSTRACT

Hydroxyapatite-associated bacterial cellulose (BC/HA) is a promising composite for biomedical applications. However, this hybrid composite has some limitations due to its low *in vivo* degradability. The objective of this work was to oxidize BC and BC/HA composites for different time periods to produce 2,3 dialdehyde cellulose (DAC). The BC and oxidized BC (OxBC) membranes were mineralized to obtain the hybrid materials (BC/HA and OxBC/HA) and their physico-chemical, degradability, and bioactivity properties were studied. The results showed that OxBC/HA was more bioactive and degradable than BC/HA, which isa function of the degree of BC oxidation. High glucose levels in the BC degradation were observed as a function of oxidation degree, and other products, such as butyric acid and acetic acid resulted from DAC degradation. Therefore, this chemical modification reaction favors BC degradation, making it a good biodegradable and bioactive material with a potential for bone regeneration applications.

1. Introduction

Bacterial cellulose (BC) is a linear polymer composed of β-D-glucopyranose units synthesized extracellularly by non-pathogenic bacteria, especially those of the genus *Komagataeibacter*. In contrast to a vegetable cellulose, BC is free of hemicellulose, lignin, and other types of impurities (Tanskul, Amornthatree, & Jaturonlak, 2013). This biopolymer has characteristics such as high purity, crystallinity, porosity, mechanical strength, humidity, hygroscopicity, biocompatibility, and good chemical stability, which makeBC a highly versatile biopolymer used in different industrial fields (Mohite & Patil, 2014; Rajwade, Paknikar, & Kumbhar, 2015).

The combination of natural polymers with organic or inorganic materials has been proposed for regenerative medicine, to develop composites with improved properties, such as antimicrobial activity and tissue regeneration capacity (Armentano et al., 2018; Jesus, Pellosi, & Tedesco, 2019). Among these combinations, previous studies have described the association between BC and hydroxyapatite (HA), obtaining composites with biocompatible properties for the osteoblastic and the stromal cells of the bone marrow (fibroblasts, macrophages, endothelial cells, and adipocytes), which favors its use for bone regeneration (Luz et al., 2018; Niamsap, Lam, & Sukyai, 2019; Saska

* Corresponding author at: Departamento de Engenharia Química, Bloco 709, Campus do Pici, Fortaleza, Ceará, Brazil.
E-mail addresses: erikapatriciagomes@alu.ufc.br (E.P.C.G. Luz), paulohiago2011@hotmail.com (P.H.S. Chaves), lidia_vieira@uol.com.br (L.d.A.P. Vieira), sadwa.fernandes@hotmail.com (S.F. Ribeiro), maria.fatima@embrapa.br (M.d.F. Borges), fabiakarine@gmail.com (F.K. Andrade), celli.muniz@embrapa.br (C.R. Muniz), ainfantes@uma.es (A. Infantes-Molina), castellon@uma.es (E. Rodríguez-Castellón), morsyleide.rosa@embrapa.br (M.d.F. Rosa), rodrigo@gpsa.ufc.br (R.S. Vieira).

https://doi.org/10.1016/j.carbpol.2020.116174
Received 9 January 2020; Received in revised form 10 March 2020; Accepted 13 March 2020
Available online 17 March 2020

et al., 2011).

Despite its properties as a promising polymeric matrix, there are some drawbacks in BC structure that restricts its use for bone regeneration applications, particularly its *in vivo* non-degradability (Hu et al., 2016; Li, Wan, Li, Liang, & Wang, 2009). In this case, the produced bone-grafting material must be degraded for complete bone repair and formation.

Several functionalization techniques using raw cellulose structure have been described to tailor its properties for specific applications. Various esterification, etherification, oxidation, copolymerization, and grafting and crosslinking reactions have been performed on the cellulose backbone. In this work, we have focused on oxidized BC (OxBC), since it is a process that does not alter the polymeric skeleton and occurs partially or totally by means of covalent bonds, involving the conversion of alcoholic groups to carbonyl or carboxyl groups (Klemm, Philipp, Heinze, Heinze, & Wagenknecht, 1998). A strong oxidizing agent, $NaIO_4$, was used in an aqueous medium, producing periodate ions that interact with BC by an electrostatic attraction. These periodate ions are specific oxidants that can oxidize the vicinal alcoholic groups at carbon atoms 2 and 3 in an anhydroglucose unit of cellulose, forming two aldehyde groups and a cellulose derivative known as 2,3-dialdehyde cellulose (DAC) (Coseri et al., 2013).

This process generates a material with adequate properties, especially for a guided bone regeneration (GBR). For this technique, it is interesting to use degradable materials, avoiding the possibility of a second surgery, reducing the psychological stress of the patient as well as the risks of new infections to the implant site and the regenerated tissue (Hou et al., 2018).

The insertion of active components, such as HA, may also be beneficialfor potentialization of bone regeneration. Successful bone tissue regeneration requires developing a matrix that provides structural support for fixation, spread, migration, proliferation, and differentiation of developing tissue. An important parameter is the material bioactivity, which is the ability to induce calcification by anucleation of calcium and phosphate crystals on its surface (Ribeiro et al., 2015).

The objective of this work was to oxidize the BC membranes to different degrees, obtain DAC or OxBC, and produce a hybrid material, OxBC/HA. These materials were characterized based on their chemical structure, morphology, surface composition, crystallinity, and swelling degree. The effect of degree of oxidation on *in vitro* material degradability properties was also evaluated. The main degradation products and mineralization phenomena were quantified by high performance liquid chromatography (HPLC) and surface analyses, respectively.

2. Materials and methods

2.1. BC synthesis and purification

BC was obtained from *Komagataeibacter hansenii* ATCC 53582 culture. Initially, inoculation of stock samples containing inclined agar was carried out and a portion of cell mass was removed by scattering on the surface of a centrifuge tube 50 mL containing Hestrin Agar and Scharmm HS (Hestrin & Schramm, 1954). In this process, the microorganism activation occurred at 30 °C for 3 days. Thereafter, a portion of cell mass removed was placed in a Scott vial containing 100 mL of the HS synthetic medium and incubated at 30 °C for 3 days. Thereafter, 5% (v/v) inoculum was with drawn and added into Scott flasks with 100 mL of HS liquid medium, and incubated for 5 days at 30 °C. The BC membranes were synthesized and purified according to previously described protocols (Luz et al., 2018).

2.2. Cellulose oxidation

The oxidation was performed by immersing the purified BC in KCl–HCl (pH 1) for 12 h. The oxidation was carried out following these experimental ratios: BC/$NaIO_4$ (1.0 g/1.5 g) and BC/KCl–HCl (0.356 g/50 mL). BC was added to the reaction system containing KCl–HCl and $NaIO_4$ pre-warmed at 55 °C and soaked (125 rpm) for 6 h, 16 h, and 24 h. The system was then incubated with 12.5 mL ethylenglycol at 25 °C for 1 h to decompose the remaining periodate and stop the reaction. It was subsequently successive washed with deionized water until membrane neutralization was achieved.

2.3. Synthesis of OxBC/HA composite membranes

The oxidized BC were soakedin 0.1 mol/L $CaCl_2$ solution for 24 h,followed by an immersion in 0.06 mol/L of Na_2HPO_4 solution for 24 h under stirring, as described by Luz et al. (2018).

2.4. Characterization of the materials produced

2.4.1. Oxidation degree by titration method

Oxidation with $NaIO_4$ converted the alcoholic groups (C—OH) into aldehyde groups (R—CH═O). The oxidized BCs (~0.25 g) were immersed in 0.1 L of 0.75 mol/L NH_2OH–HCl solution at pH 5, and incubated for 18 h at 40 °C under stirring. The samples were titrated using 1 mol/L NaOH solution. The oxidation degree was determined using the direct relationship between the volume of NaOH spent and aldehyde content (AC) formed, as described by Li et al. (2009).

2.4.2. Swelling degree

Samples (10 × 10 mm^2) were immersed in distilled water (pH 7.1) for 0 min, 1 min, 2 min, 7 min, 12 min, 22 min, and 32 min at 25 °C. Afterwards, the membranes were removed from water; the excess water was removed using filter paper (Quanty; 8 μm) and weighed. The swelling degree was expressed as the percentage of weight gained compared to the dry weight.

2.4.3. Scanning electron microscopy (SEM)

The samples were previously lyophilized and carefully placed on metal supports, with the help of a double-sided carbon tape. Then, metallization was performed with the deposition of an approximately 30 nm thick conductive gold layerby sputtering, using a metallizer (K650; Emitech; France). The micrographs were obtained using a scanning electron microscope (DSM 940; Zeiss; Germany) with a voltage of 15 kV.

2.4.4. X-ray diffraction (XRD)

The XRD patterns were obtained using a diffractometer for polycrystalline samples (XPert Pro MPD – Panalytical, Netherlands) with a Cu tube at 40 kV and 40 mA at 2θ scale. The angular range used ranged from 3°–50°, with a scanning speed of 0.5°/min. The crystallinity index (CI) was estimated as described by Segal, Creely, Martin, and Conrad (1959) using Eq. (1).

$$CI(\%) = \left(\frac{I_{002} - I_{am}}{I_{002}}\right) \times 100 \quad (1)$$

where I_{002} and I_{am} is are the intensitiesof crystalline cellulose at $2\theta^{\circ} - 23^{\circ}$ and is the amorphous cellulose at $2\theta^{\circ} - 17^{\circ}$, respectively.

2.4.5. Fourier transform infrared spectroscopy (FTIR)

The FTIR analyses were performed using the attenuated total reflectance (ATR) method in a spectrophotometer (660 Varian; United Kingdom) with a reading range of 4000 cm^{-1} – 400 cm^{-1} with a resolution of 4 cm^{-1} and 15 scans.

2.4.6. Solid state nuclear magnetic resonance (NMR)

^{13}C MAS NMR spectra were recorded at room temperature (25 °C) with an AVANCEIII HD 600 spectrometer (Bruker; USA) using an HXY, Efree MAS probe of 3.2 mm at a spinning rate of 15 kHz. The magnetic field was 14.1 T, corresponding to a ^{13}C resonance frequency of

150.9 MHz. All spectra were recorded using a Cross Polarization Magic-Angle Spinning (CP-MAS) pulso program: a combination of cross-polarization, high-power proton decoupling, and magic angle spinning. The ^{13}C chemical shift values were measured with respect to glycine as a secondary reference (carbonyl signal at 176.03 ppm).

2.4.7. X-ray photoelectron spectroscopy (XPS)

XPS spectra were collected using aspectrometer (PHI Versaprobe II Scanning XPS Microprobe; Physical Electronics; USA) with monochromatic X-ray Al Kα radiation (100 μm, 100 W, 20 kV, 1486.6 eV) and a dual-beam charge neutralizer. XPS spectra were analyzed using PHI SmartSoft software and processed using the MultiPak 9.3 package. The binding energy values were referenced to the adventitious C 1*s* signal at 284.8 eV. Recorded spectra were fitted using the Gaussian–Lorentz curves. The atomic concentration percentages of the constituent elements of the surfaces were determined considering the corresponding area sensitivity factor for the different measured spectral regions.

2.4.8. Thermogravimetric analysis (TGA)

The TGAs were conducted using approximately 7.0 mg of each sample between 0 °C and 700 °C at a heating rate of 10 °C/min under a nitrogen atmosphere with a flow rate of 40 mL/min in a thermogravimetric analyzer (TGA-50; Shimadzu; Japan).

2.5. In vitro degradability test

For the *in vitro* degradation test, the samples were immersed in phosphate-buffered saline solution (PBS) for 15 days, 30 days, 60 days, and 90 days using a static condition in a Biochemical Oxygen Demand (BOD) incubator at 37 °C. The degraded product was removed from the supernatant and analyzed by HPLC using an AMINEX HPX-87H column (Bio-Rad; Hercules, CA, USA) at 65 °C and 0.005 mol/LH_2SO_4 in MilliQ water as the mobile phase with a flow rate of 0.6 mL min^{-1}. The freeze-dried samples were cut into cubes (10 × 10 mm^2), weighed, placed in a 50 mL centrifuge tube containing 0.01 L PBS, and incubated at 37 °C.

2.6. Bioactivity test

The bioactivity was evaluated using energy dispersive X-ray (EDX) analysis to verify the ability of the material to induce an apatite formation on its surface when immersed in PBS, whose ionic concentrations were approximately equal to those of the human blood plasma (Bohner & Lemaitre, 2009). The samples were freeze-dried, placed in stubs, covered with a thin gold layer, and visualized using a scanning electron microscope (Inspect-50; Japan) with a voltage of 15 kV.

3. Results and discussion

3.1. BC weight loss

The oxidation were performed for three different time periods and the weight loss during the production of BC derivatives was investigated. During oxidation, a part of the material is solubilized, increasing weight loss with reaction time increase. The results showed mass losses of 8%, 50 %, and 66 % for OxBC 40 %, OxBC 60 %, and OxBC 90 % OxBC, respectively. After the reaction, the products of alcohol oxidation to carbonyl groups on the BC structure becomes insoluble in water but remains soluble in solvents, such as HCl used in oxidation.

3.2. Swelling degree

These experiments were performed to investigate the effect of oxidation on the swelling polymer matrix. Fig. 1A shows that the sample equilibrium was achieved in a short time, approximately 22 min, and decreased by increasing the oxidation degree from 40 % to 90 %. These results were found to agree with those previously described, which showed that the OxBC samples were more hydrophobic than native BC, probably due to the formation of aldehyde groups, decreasing hydrogen bonds with the hydroxyl groups on the BC structure (Hutchens et al., 2009). These results were similar to those reported by Yang, Zhen, Che, and Shan (2016). Fig. 1B shows that the BC/HA and OxBC/HA swelling equilibrium was achieved at a high equilibrium time. This characteristic is associated with the hydrophilic character of HA in the production of composite matrices (Luz et al., 2018).

3.3. SEM

Fig. 2 shows the microscopy surfaces of the native and the oxidized bacterial cellulose samples. Nanofiber uniformity was observed in the BC samples. The average fiber diameter was 50 nm ± 1 nm, confirming the nanometric dimensions. In the 40 % OxBC sample, a slight change in texture was detected, but the structure was preserved with some nanofibers. For the samples with a high oxidation degree (60 % and 90 %), a dense and compact cellulose nanofiber network structure was observed, with some ruptures in the nanofiber surface layer, suggesting fragility in the fibers and probably a decrease in the crystalline structure.

It was observedthat both BC/HA and OxBC 40 %/HA samples had similar morphological behavior, indicating that this slight oxidation did not modify the polymer structure, generating the same HA agglomerates on BC samples. However, it was not possible to accurately identify the BC nanofibers in OxBC 60 %/HA and OxBC 90 % /HA because of their high compaction and uniform HA deposition. Hutchens et al. (2009) have proposed that calcium ions can bind to the aldehyde groups of oxidized cellulose by a strong chemical bond and potentialize the chemical stability. It has been suggested that calcium nanoparticles can be deposited in different forms of HA, explaining the limitation of identifying them by SEM images.

3.4. XRD

XRD analyses were performed to determine the effect of oxidation on material crystallinity. The X-ray diffractograms for the BC and OxBC samples have been shown in Fig. 3.

It was observed that the diffractograms (Fig. 3A) depicted three evident peaks for all the samples. The peaks at approximately 16.9° and 26.5° indicate the presence of type I cellulose and the peak near 18.5° indicate amorphous cellulose (Keshk & Sameshima, 2006; Kronenthal, 1975). It was also observed that the crystallinity index reduced with an increase in the oxidation content. These values were calculated using eq. (A.3): BC (78 %), 40 % OxBC (71 %), 60 % OxBC (61 %), and 90 % OxBC (27 %). These results confirm that crystallinity reduction occurred as a function of oxidation, as reported by Li, Wu, Mu, and Lin (2011). This phenomenon resulted from the opening of the glucopyranose rings and destruction of their ordering structure (Li et al., 2009). Previous studies suggest that three reactions occur simultaneously during periodate oxidation: a rapid initial attack of the periodate in the amorphous region of the cellulose, a second slow reaction attributed to the oxidation of the surface of the crystalline regions, and a third very slow reaction due to the oxidation of the crystalline nucleus (Calvini, Gorassini, Luciano, & Franceschi, 2006). In the composite diffractograms (Fig. 3B), diffraction peaks attributed to the type I standard cellulose were found in regions A and B as there was a decrease in the intensity of these peaks, indicating that HA was the dominant component (Hutchens et al., 2009).

HA pattern peaks were observed in C, D, E, F, G, H, I, and J regions as shown in Fig. 3B (Hutchens et al., 2009). The crystallinity index of BC/HA (86 %), OxBC 40 %/HA (84 %), OxBC 60 %/HA (79 %), and OxBC 90 %/HA (68 %) composites indicated that HA made the materials more crystalline than those observed with the BC and OxBC composites.

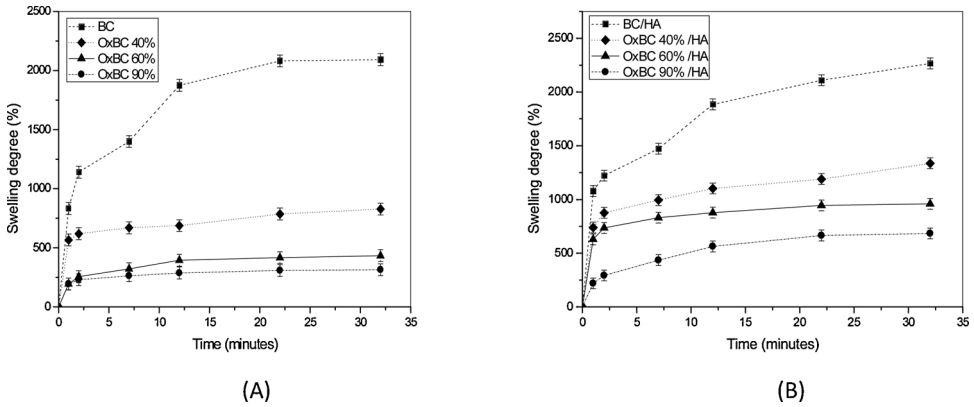

Fig. 1. Swelling degree (%) of (A) BC and its oxidized derivatives (OxBC 40 %, OxBC 60 %, OxBC 90 %) and (B) BC/HA composites with different oxidation degrees (OxBC 40 %/HA, OxBC 60 %/HA, OxBC 90 %/HA).

3.5. FTIR

In the spectra referring to BC (Fig. 4A), characteristic BC vibrational bands were identified at 3353 cm^{-1} (stretching of the −OH bond), 2897 cm^{-1} (symmetrical stretch of C−H group), 1645 cm^{-1} (referring to the bending deformation of −C−OH), and 1000–1600 cm^{-1} (low-intensity bands attributed to C−H groups in cellulose) (Sun, Hou, Liu, & Ni, 2015). It could also be observed that the intensity of the bands related to the stretching of the OH bond (3353 cm^{-1}) decreased with an increase in the oxidation degree, which could be explained by the conversion of hydroxyl into carbonyl groups (presented by the band at 2897 cm^{-1}) by oxidation, and in accordance with the previously reported results (Sun et al., 2015).

All the spectra present vibrational bands characteristic of BC; however, in the spectrum of the oxidized hybrid materials (Fig. 4B), these bands were attenuated, which may be due to HA deposition on the polymer surface (Hu et al., 2016). A reduction in the intensity of some bands, mainly around 3350 cm^{-1}, 1640 cm^{-1}, and 2897 cm^{-1}, were identified according to the increase of oxidation degree, possibly due to HA deposition on the polymeric surface. These results suggested that oxidation altered the molecular structure of the material, due to the conversion of alcohol groups into carbonyl groups, as reported in previous studies (Li et al., 2009; Yang et al., 2016). New bands appeared in the hybrid materials at around 1020 $cm^{-1}$and 960 cm^{-1} (referring to the phosphate groups), which decreased with the oxidation degree, suggesting that the introduction of aldehyde groups affect mineral deposition. Hutchens et al. (2009) showed a low HA concentration in OxBC samples, suggesting that the chemical modification of the cellulose network contributed to some restrictions in calcium and phosphate salt diffusion. Aldehyde has been suggested to affect an apatite nucleation, preventing HA from depositing in the DAC portions. Yang et al. (2016) suggested that oxidation elevated the anionic character of BC, allowing dipolar bonds between aldehyde clusters and Ca^{2+} ions, influencing the interaction of calcium with phosphorus to form HA.

3.6. Solid state NMR

^{13}C CP-MAS profiles (Fig. 5) showed the characteristic peaks of cellulose. In general, it clearly showed the peaks in the range 60 ppm – 70 ppm associated with C6 carbon, between 70 ppm–80 ppm assigned with C2, C3, and C5 carbons, and from 80 ppm to 905 ppm corresponding to the C4 carbon (Idström et al., 2016). Signals at low shifts, especially those of C4 and C6, indicate amorphous regions (Lemke, Dong, Michal, & Hamad, 2012). After oxidation, the signals are broadened, which can be associated with a crystallinity loss, since high resolution and sharp peaks usually imply high crystallinity. The broadened signals were noticeable in OxBC 60 % and OxBC 90 % samples, where a new broad contribution close to 100 ppm was also related to the C1 carbon. Andersson, Hoffman, Nahar, and Scholander (1990) assigned a peak at 93 ppm to C1 of the terminal α-D-glucose unit that appeared when cellulose was oxidized with sodium nitrite in orthophosphoric acid C2 and C3 signals affected by aldehyde formation were also less defined and there were no peaks due to the formation of carbonyl carbons of ketones (200 ppm – 210 ppm), resulting from the oxidation of C2 or C3 secondary hydroxyl groups (Isogai & Kato, 1998). Similar observations were obtained by Jiang, Wu, Han, and Zhang (2017) when treating cellulose with ammonium persulfate. This suggests that C2 or C3 have not been oxidized; if oxidized, the crystallinity of the resultant material will bequite low to determine the formation of these groups by NMR. These results suggest that oxidation mainly affects the crystallinity of the samples.

3.7. XPS

Oxidized BC membranes were evaluated using XPS. The C1*s* and O1*s* core level spectrawere studied to analyze the relationship between oxygen and carbon and the oxidation reaction (Fig. 6). The C1 level spectra can be decomposed into fourcontributions with maxima at approximately 284.8 eV, 286.4 eV, 287.8 eV, and 289.1 eV. The first contribution (C1) is assigned to −C−H, −C−C, and −C=C bonds mainly from an adventitious carbon.

The second contribution (C2) corresponds to −C−OH, −C−O−C,and −C−NH_2 bonds, while the third contribution (C3) is attributed to −C=O groups and the fourth contribution at a high binding energy (C4) can be assigned to the carboxylic groups (Briggs, 1981).

Fig. 6 shows the deconvoluted C1*s* core level spectra of OxBC 40 %, OxBC 60 %, and OxBC 90 % samples. The contribution of C1 in all spectra, assigned to the adventitious carbon contamination, present different relative intensities, and these intensities are independent of the oxidation degree. To follow the surface oxidation of the samples, C2/(C3 + C4) area ratios must be considered where the contribution C2 corresponds to the C−OH and C−O−C bonds from cellulose, and C2 and C3 contribute to the oxidized groups, C=O and O=C−O^-, respectively. The C2/(C3 + C4) area ratios were 2.37, 2.07,and 1.55 for the OxBC 40 %, OxBC 60 %, and OxBC 90 %, respectively. These results clearly confirm the surface oxidation of the alcoholic group of cellulose. The O1*s* core level spectra of OxBC 40 % and OxBC 60 % samples (data not shown) exhibit one symmetric peak centered at 532.8 eV, indicating that this binding energy value is similar to that found in the literature for cellulose (Dolinina, Vlasenkova, & Parfenyuk, 2017). This peak is broad and should include the −C−O−C and/or C=O and C−OH groups. In OxBC 90 % sample, the O1*s* spectrum can be decomposed into two contributions at 531.5 eV (6%) and 532.9 eV (94 %). The contribution at a low binding energy is assigned to oxygen from carboxylic, and the more intense contribution to the C−O−C and / or C=O

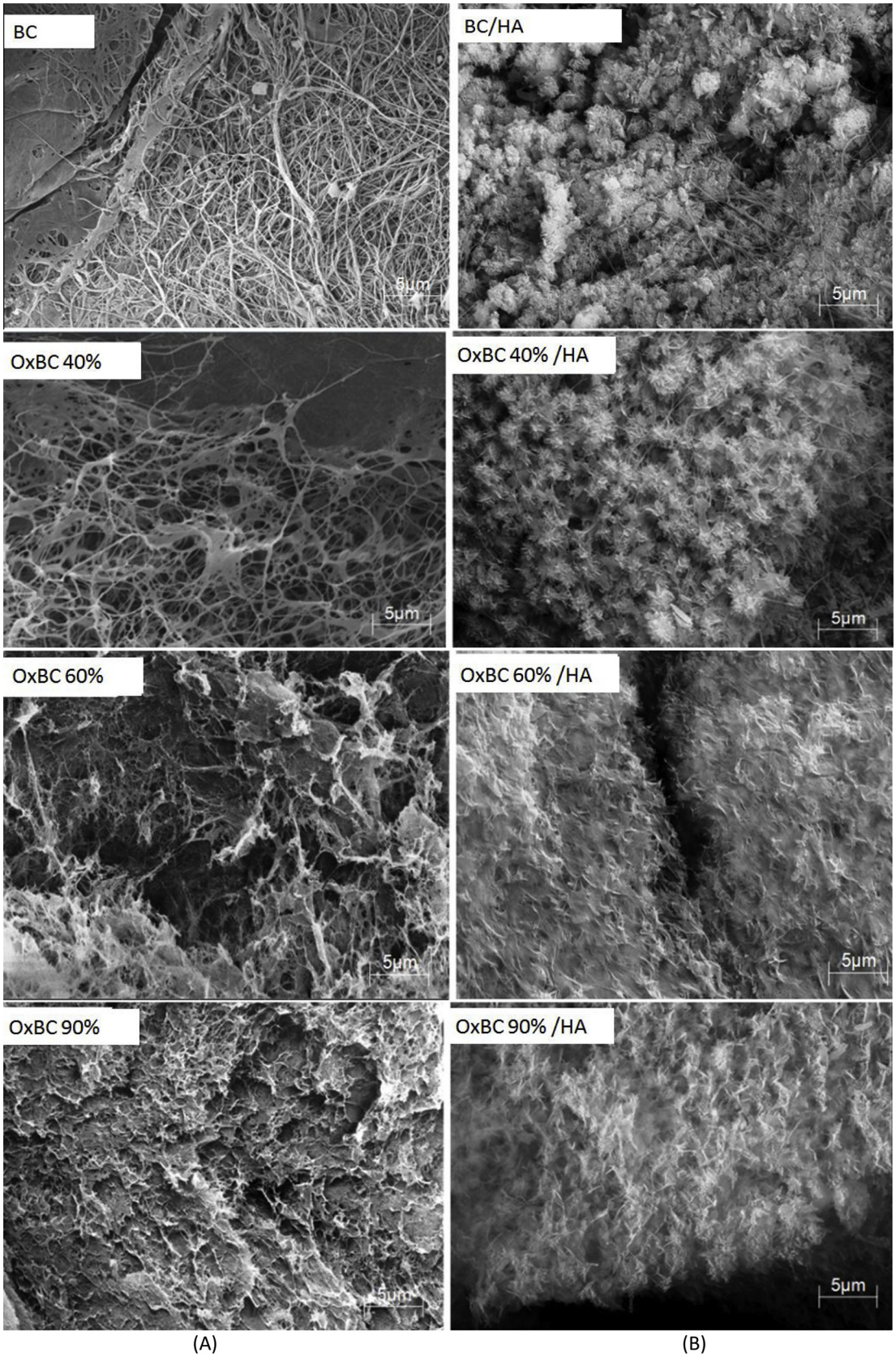

Fig. 2. Scanning electron microscopy for (A) BC and its oxidized derivatives (OxBC 40 %, OxBC 60 %, OxBC 90 %) and (B) BC/HA and composites with different oxidation degrees (OxBC 40 %/HA, OxBC 60 %/HA, OxBC 90 %/HA).

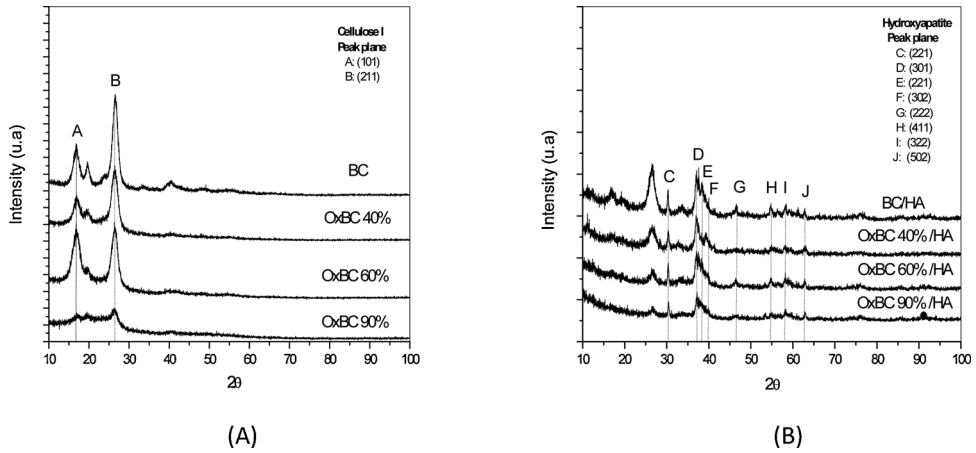

Fig. 3. X-Ray diffractograms for (A) BC and its oxidized derivatives (OxBC 40 %, OxBC 60 %, OxBC 90 %) and (B) BC/HA and composites with different oxidation degrees (OxBC 40 %/HA, OxBC 60 %/HA, OxBC 90 %/HA).

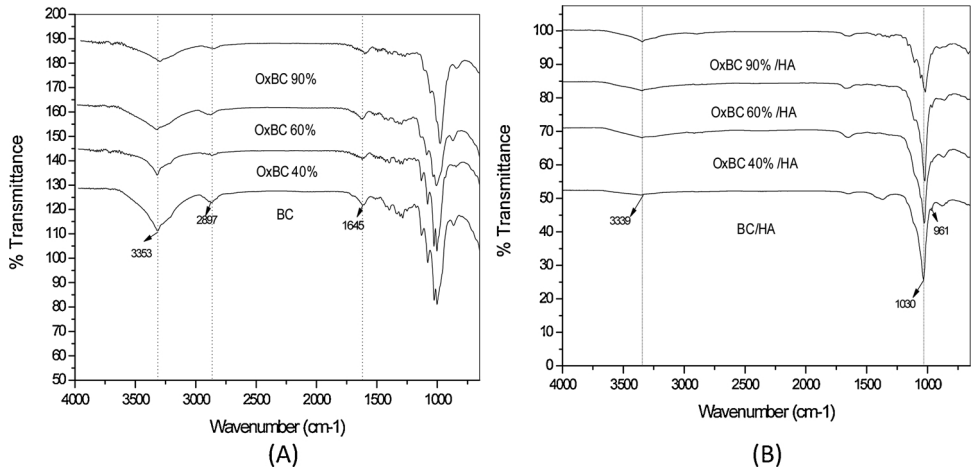

Fig. 4. Vibrational spectra in the infrared region for (A) BC and its oxidized derivatives (OxBC 40 %. OxBC 60 %, OxBC 90 %) and (B) BC/HA composites with different oxidation degrees (OxBC 40 %/HA. OxBC 60 %/HA, OxBC 90 %/HA).

and C—OH groups.

The experimental O/C ratio of OxBC samples were (0.70) OxBC 40 %, (0.60) OxBC 60 %, and (0.46) OxBC 90 %. The XPS results showed that the longer the membrane was subjected to oxidation, the lower was its O/C ratio. The theoretical value for pure cellulose is 0.83, according to Topalovic et al. (2007). The decrease in this ratio is related to the degradation and possible loss of oxygen atoms during oxidation, corroborating the BC mass loss, since during oxidation there is a mass reduction due to this modification occurring in an acidic environment that may cause material degradation; therefore, it does not guarantee the same proportions of the elements O and C present in the BC.

3.8. TGA

The thermogravimetric curves for BC and its oxidized derivatives have been shown in Fig. 7A. From these curves, a first event of weight loss (3%–7%) was observed at about 100 °C for volatile compounds. In the second event, the weight loss occurred due to the processes of cellulose degradation, such as depolymerization, dehydration, and glycosidic unit decomposition. The third event at about 400 °C to 700 °C could be correlated to the formation of carbon residues (Duarte et al., 2015). By the derivation of thermogravimetric (DTG) curves (Fig. 7B), it was possible to identify the maximum temperature degradation for each sample. It was observed that the OxBC 90 % sample showed two degradation peaks, probably due to the high oxidation degree, resulting in a fractional degradation of the material (Siller et al., 2015). Although oxidation decreases the thermal stability, this does not limit the type of application as the material is capable of with standing autoclave sterilization temperatures, and degradation processes occur at much higher temperatures than sterilization processes.

The TGA of the BC composites with different degrees of oxidation and Ca–HA (Fig. 7C) also showed a gradual reduction in degradation temperature, according to the increase in the oxidation degree as well as in BC and its oxidized derivatives. However, due to the interactions between HA and the samples, a high deviation was observed in terms of the percentage values of residues at 700 °C. The non-oxidized composite presented a lower degradation temperature than that by the non-oxidized BC because of HA deposition on its surface (Ahn et al., 2015). The results obtained (Fig. 7D) show a reduction in loss of mass due to thermal stability asa function of the interaction between the samples and HA (Ahn et al., 2015; Hu et al., 2016).

3.9. In vitro degradability test

The degradation of composite membranes was quantified by HPLC, measuring the amount of glucose (fundamental BC unit) in the PBS supernatants. Fig. 8 shows the mechanism for hydrolytic degradation of oxidized cellulose, producing 2,4-dihydroxybutyric acid, glycolic acid (or hydroxyacetic acid), and carbohydrates (Hutchens et al., 2009). The BC samples showed a low level of degradation, as explained by Li et al. (2009), who described that BC degradation in the body was very low and increased by chemical modifications such as oxidation.

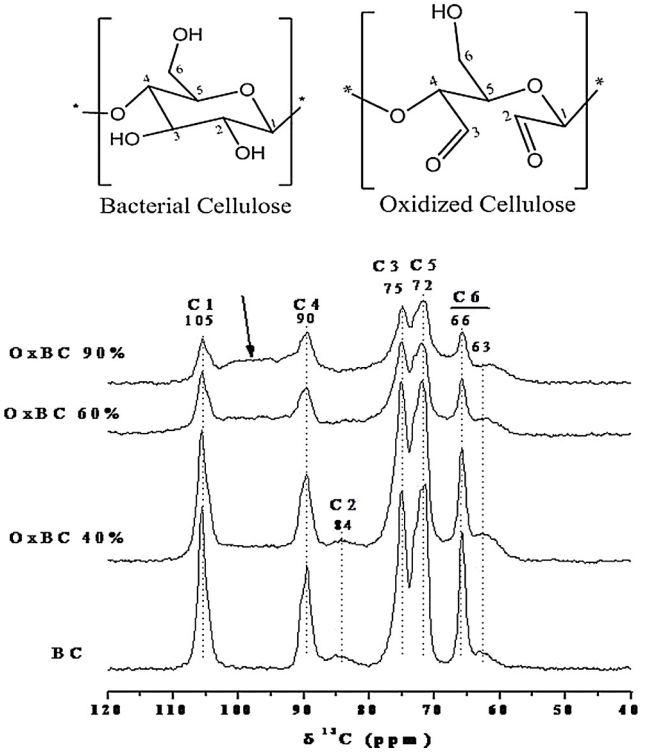

Fig. 5. ^{13}C NMR spectra of BC and OXBC samples.

The results showed an increase in glucose concentration with increase in the oxidation degree. As hypothesized, in addition to glucose, OxBC degradation products, identified as butyric acid and acetic acid, were also found for some samples. This degradability can be an important requirement for guided bone regeneration, since it can be modulated inside the body.

Comparing Fig. 9A and B, it was observed that glucose concentration in the composites was lower than that in the BC samples, suggesting that hybrid materials conferred some chemical stability to the final product, corroborating the FTIR, SEM, and TGA results. This increase in stability can be attributed to the isolated pairs in the aldehyde groups that coordinate the calcium ions, forming a strong chemical bond and decreasing the degradability rate.

OxBCs degrade faster than oxidized composites, which may be an interesting focus for tissue engineering. For cases where a long material permanence is required, the use of composite as a controlled release system is more appropriate, while for use as a carrier for drugs where fast degradation is required, OxBC is the most appropriate choice.

Earlier studies have reported that HA is stable under physiological conditions. In this study, we used a mildly basic pH of 7.4, which did not degrade HA. However, some *in vivo* studies have shown HA breakdown due to the response of an organismto a foreign component, lowering the medium pH to a range of 4–5 locally, which is considered the initial inflammation pH (Habraken, Habibovic, Epple, & Boher, 2016). HA dissolves in this pH range and is subsequently absorbed by the individual. Noteworthy, in bone regeneration studies with active osteoclastic cells, they release H^+ ions, making the physiological environment acidic (Seo, Ryu, Park, Huh, & Baek, 2016).

3.10. Bioactivity test

To evaluate the potential of materials for use in bone regeneration, a bioactivity test was performed to identify the ability of the samples to induce calcification. Material bioactivity is identified by the ability of the biomaterial to establish a stable bond with living tissues *via* an HA deposition (Czarnecka, Coleman, Shaw, & Nicholson, 2008). According to Duarte et al. (2015), HA precipitation on the material surface exposed *in vitro* to simulated body fluid (SBF) solution indicates a bioactivity.

Microanalysis using an EDX detector was performed to quantify the surface chemical composition and describe if the material has potential bioactivity. It compared BC samples and their oxidized derivatives, as well as the composites of BC with different oxidation degree and HA (Table 1) after being immersed in SBF for 15 days, to identify a possible interaction with the SBF medium causing the deposition of ions such as calcium and phosphorus.

Only carbon and oxygen, the fundamental elements of cellulose, were present in BC and its oxidized derivatives. However, calcium and phosphorus was also detected in the BC composites with different degrees of oxidation and HA, forming HA elements. Chlorine and sodium

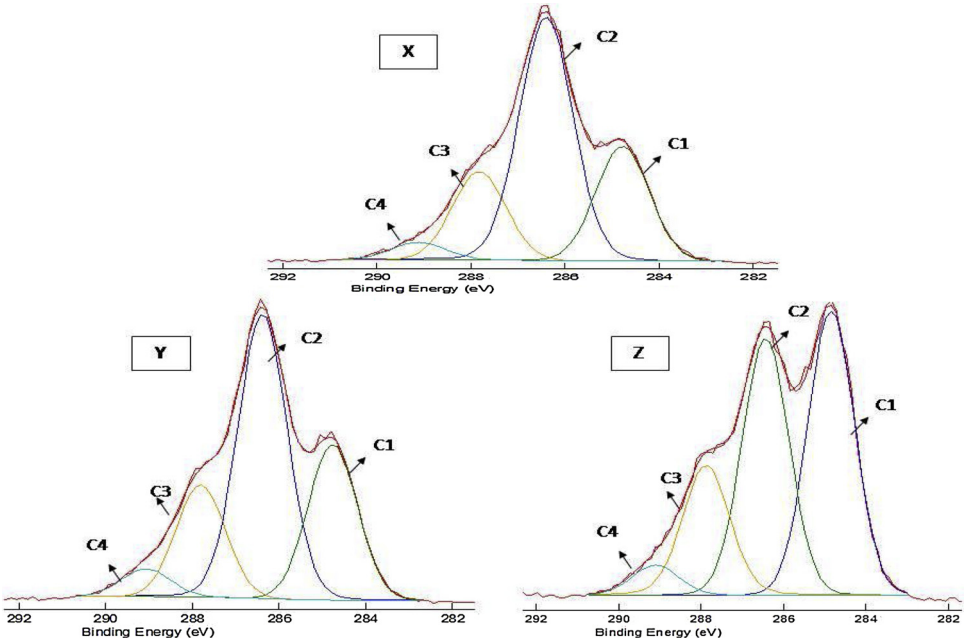

Fig. 6. C1*s* core level spectra corresponding to X) OxBC 40 %, Y) OxBC 60 %, and Z) OxBC 90 %.

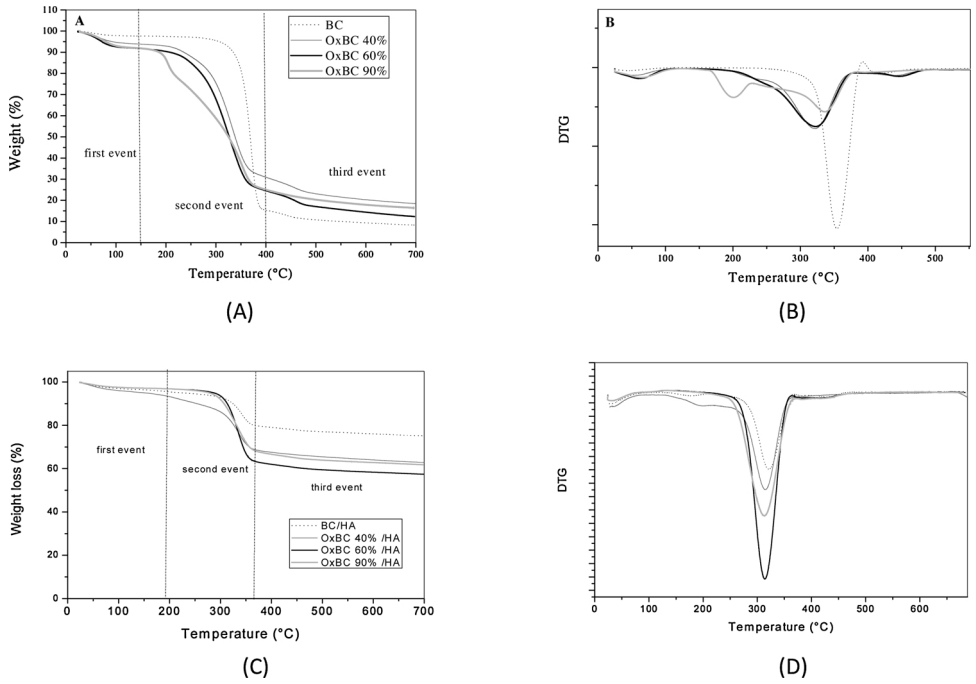

Fig. 7. Thermogravimetric analysis (TGA/DTG) of (A, B) BC and its oxidized derivatives (OxBC 40 %, OxBC 60 %, OxBC 90 %) and (C, D) BC/HA and composites with different degrees of oxidation (OxBC 40 %/HA, OxBC 60 %/HA, OxBC 90 %/HA).

was also detected in smaller quantities, derived from the solutions used for producing the hybrids ($CaCl_2$ and Na_3PO_4). The predominance of carbon and oxygen (Table 1) in the elemental composition of these samples confirms its cellulosic nature. There were small variations in the percentage of these elements among the samples, probably due to the area chosen for the analysis.

Comparing the calcium values before and after immersion in SBF,calcification was observed for the OxBC 60 % and OxBC 90 % samples, demonstrating that the polymeric matrix favored an HA deposition, which was related to the cellulose chain hydroxyl clusters, confirming the minetic route for producing the hybrid BC/HA according to Li et al. (2009). For the composites, interaction with the SBF medium was identified, causing calcium release and deposition mechanisms, as exemplified in the results of BC/HA and OxBC/HA 90 %, respectively.

The hybrids mostly interacted with the SBF medium, indicating that HA presence in the material optimized the calcification in the material, making it more bioactive. Besides being more bioactive with higher oxidation degree, the hybrid materials formed by oxidized matrices are degradable and useful for successful bone tissue engineering. It is essential that the implanted graft materials should have an appropriate cell affinity and be potentially degradable. The calcification process is correlated to the surface characteristics of the material, which may be related to the chemical composition, which causes a process of complexation of chemical groups on the surface of the material, with calcium or phosphorus ions leading to an apatite nucleation or due to roughness, contributing to an ionic anchorage in their pores (Ribeiro et al., 2015).

For the composites, the Ca/P ratios were calculated, which can be used to characterize the composition of calcium phosphates (Habraken et al., 2016). Traces of chlorine and sodium, probably residues from the reagents used in the mineralization were identified. The formula for stoichiometric HA is $Ca_{10}(PO_4)_6(OH)_2$, with a Ca/P ratio of 1.67, which is the most stable and least soluble calcium phosphate of all (Duarte

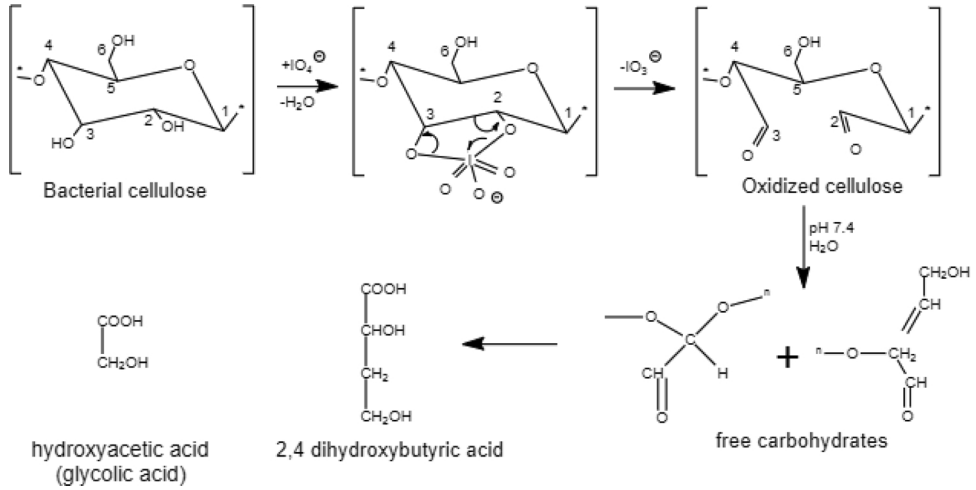

Fig. 8. Scheme of bacterial cellulose oxidation by sodium periodate and mechanism for hydrolytic degradation of oxidized cellulose producing carbohydrates, 2,4-dihydroxybutyric acid and glycolic acid (or hydroxyacetic acid),proposed by Hou et al. (2018).

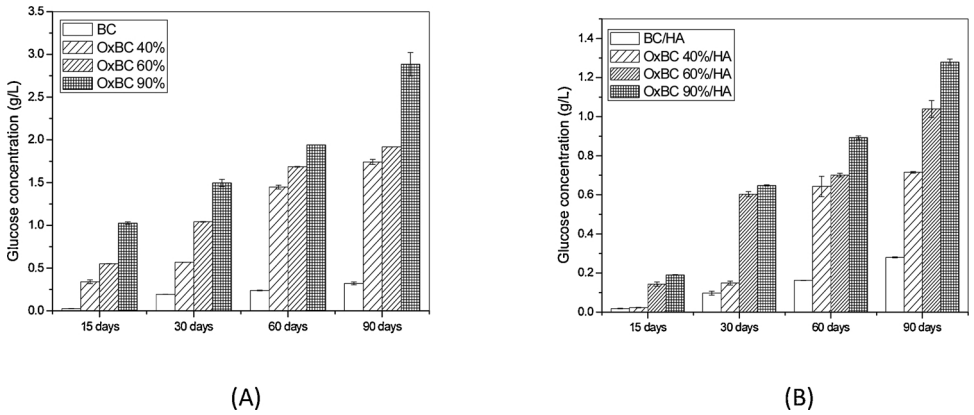

Fig. 9. Values of glucose concentration by *in vitro* degradability time in PBS for (A) BC and its oxidized derivatives and(B) BC/HA with different oxidation degrees.

Table 1
Surface chemical analysis by EDX for all BC samplesbefore and after SBF immersion.

Sample	C (%)	O (%)	Ca (%)	P (%)	Na (%)	Cl (%)
[bf] BC	72.7	27.3	–	–	–	–
[*bf] OxBC 40%	72.7	27.3	–	–	–	–
[*bf] OxBC 60%	72.7	27.3	–	–	–	–
[*bf] OxBC 90%	72.7	27.3	–	–	–	–
[*bf] BC/HA	8.5	50.4	21.5	13.5	5.5	0.6
[bf] OxBC 40%/HA	12.5	55.0	16.8	10.3	4.9	0.5
[bf] OxBC 60%/HA	18.1	62.0	18.1	11.3	1.8	0.1
[bf] OxBC 90%/HA	11.7	54.2	23.1	10.5	0.3	0.1
[af] BC	60.5	39.3	–	0.1	–	0.1
[af] OxBC 40%	56.7	43.1	–	–	–	0.2
[af] OxBC 60%	47.1	52.6	0.1	–	0.1	–
[*af] OxBC 90%	50.6	48.7	0.5	0.1	–	0.2
[af] BC/HA	6.8	55.8	17.9	8.5	0.4	0.1
[af] OxBC 40%/HA	13.8	48.6	18.5	12.9	5.0	1.2
[af] OxBC 60% /HA	18.8	48.4	18.7	11.0	2.7	0.4
[af] OxBC 90%/HA	3.5	44.9	28.1	16.6	5.9	1.0

*bf before immersion in SBF.
*af after immersion in SBF.

et al., 2015). The Ca/P ratio in BC/HA (1.59), 40 % OxBC/HA (1.63), and 60 % OxBC/HA (1.60) was close to that in biological HA, but was higher in 90 % OxBC/HA (2.20). Calcium ion content plays a role in osteoblast adhesion and proliferation, which can be an important step towards the secretion of abone matrix mineralization and the formation of a new bone.

4. Conclusions

This work describes, for the first time, the production of hybrids based on OxBC and HA at different time periods of oxidation with respect to degradation of the material, favoring biomaterial research aimed at future applications in guided bone regeneration.

The oxidation, under the study conditions, proved to be effective for degrading the bacterial cellulose membrane, indicating that it had a direct relationship with the increase in the degree of oxidation. It has also been shown that oxidation influences the swelling and crystallinity of the material. The degree of oxidation can be controlled by the reaction time. Thus, we can conclude that oxidation is an alternative chemical modification to optimize BC degradability.

Oxidized matrix composites have been shown to be the most suitable for use in bone regeneration as they have an initial stable support for bone cells that have active components that interact with bone cells. This material slowly degrades, allowing favorable conditions for the cells to mineralize and form new bones. The special highlight of the materials produced is the ability to adjust the degradation profiles according to the degree of oxidation of the polymer matrix.

CRediT authorship contribution statement

Erika Patricia Chagas Gomes Luz: Conceptualization, Methodology, Validation, Formal analysis, Investigation, Data curation, Writing - original draft, Visualization. **Paulo Hiago Silva Chaves:** Investigation, Data curation. **Lidia de Araújo Pinto Vieira:** Investigation, Data curation. **Sádwa Fernandes Ribeiro:** Investigation, Data curation. **Maria de Fátima Borges:** Resources. **Fabia Karine Andrade:** Conceptualization, Writing - review & editing, Supervision. **Celli Rodrigues Muniz:** Resources. **Antonia Infantes-Molina:** Resources, Writing - review & editing. **Enrique Rodríguez-Castellón:** Resources, Writing - review & editing. **Morsyleide de Freitas Rosa:** Conceptualization, Methodology, Writing - review & editing, Supervision. **Rodrigo Silveira Vieira:** Conceptualization, Methodology, Writing - review & editing, Supervision, Project administration.

Declaration of Competing Interest

The authors declare that they have no conflict of interest and that themanuscript has not been published elsewhere, is not under editorial review for publication elsewhere, and is not being submitted simultaneously to another journal.

Acknowledgements

The authors would like to thank the Coordination for the Improvement of Higher Education Personnel (CAPES), National Counsel of Technological and Scientific Development (CNPq), Cearense Foundation for the Support of Scientific and Technological Development (FUNCAP), and the Embrapa Agroindústria Tropical for funding this research. This research was also supported by the following projects: FUNCAP/CNPq (PR2-0101-00023.01.00/15), CNPq (nº 305504/20169), CNPq (nº 402561/2007-4), PROCAD/CAPES (88881.068439/2014-01) and CTQ2015-68951-C3-3R (Ministerio de Economía y Competitividad, Spain and FEDER Funds). A.I.M. thanks the Ministry of Economy and Competitiveness for a Ramón y Cajal contract (RyC2015-17870).

References

Ahn, S. J., Shin, Y. M., Kim, S. E., Jeong, S. I., Jeong, J. O., Park, J. S., et al. (2015). Characterization of hydroxyapatite-coated bacterial cellulose scaffold for bone tissue engineering. *Biotechnology and Bioprocess Engineering, 20*, 948–955.

Andersson, R., Hoffman, J., Nahar, N., & Scholander, E. (1990). An N.M.R. Study of the products of oxidation of cellulose and (1,4)-β-d-xylan with sodium nitrite in orthophosphoric acid. *Carbohydrate Research, 206*, 340–346.

Armentano, I., Gigli, M., Morena, F., Argetanti, C., Torre, L., & Martino, S. (2018). Recent advances in nanocomposites based on aliphatic polyesters: Esign, synthesis, and applications in regenerative medicine. *Applied Sciences, 8*, 1452–1462.

Bohner, M., & Lemaitre, J. (2009). Can bioactivity be tested in vitro with SBF solution? *Biomaterial, 30*, 2175–2179.

Briggs, D. (1981). In C. D. Wanger, W. M. Riggs, L. E. Davis, J. F. Moulder, & G. E. Muilenberg (Eds.). *Handbook of X-ray photoelectron spectroscopy* (pp. 190). Perkin-Elmer Corp., Physical Electronics Division.

Calvini, P., Gorassini, A., Luciano, G., & Franceschi, E. (2006). FTIR and WAXS analysis of periodate oxycellulose: Evidence for a cluster mechanism of oxidation. *Vibrational Spectroscopy, 40*, 177–183.

Coseri, S., Biliuta, G., Simionescu, B., Stana, K. K., Ribitsch, V., & Harabagiu, V. (2013). Oxidized cellulose survey of the most recent achievements. *Carbohydrate Polymers, 93*, 207–215.

Czarnecka, B., Coleman, N. J., Shaw, H., & Nicholson, J. W. (2008). The use of mineral trioxide aggregate in endodontics. *Dental and Medical Problems, 45*, 5–11.

Dolinina, E. S., Vlasenkova, M. I., & Parfenyuk, E. V. (2017). Effect of trehalose on structural state of bovine serum albumin adsorbed onto mesoporous silica and the protein release kinetics in vitro. *Colloids and Surfaces A: Physicochemical and Engineering Aspects, 527*, 101–108.

Duarte, E. B., Chagas, B. S., Andrade, F. K., Brígida, A. I. S., Borges, M. F., Muniz, C. R., et al. (2015). Production of hydroxyapatite-bacterial cellulose nanocomposites from agroindustrial wastes. *Cellulose, 22*, 3177–3187.

Habraken, W., Habibovic, P., Epple, M., & Boher, M. (2016). Calcium phosphates in biomedical applications: Materials for the future? *Materials Today, 19*, 69–87.

Hestrin, S., & Schramm, M. (1954). Synthesis of cellulose by *Acetobacter xylinum*. Preparation of freeze-dried cells capable of polymerizing glucose to cellulose. *Biochemical Journal, 58*, 345–352.

Hou, Y., Wang, X., Yang, J., Zhu, R., Zhang, Z., & Li, Y. (2018). Development and biocompatibility evaluation of biodegradable bacterial cellulose as a novel peripheral nerve scaffold. *Journal Of Biomedical Materials Research Part A, 106*, 1288–1298.

Hu, Y., Zhu, Y., Zhou, X., Ruan, C., Pan, H., & Catchmark, J. M. (2016). Bioabsorbable cellulose composites prepared by an improved mineral-binding process for bone defect repair. *Journal Material Chemical, 4*, 1235–1246.

Hutchens, S. A., Benson, R. S., Neill, Evans, B. R., Neill, H. M. O., & Rawn, C. J. (2009). A resorbable calcium-deficient hydroxyapatite hydrogel composite for osseous regeneration. *Cellulose, 16*, 887–989.

Idström, A., Schantz, S., Sundberg, J., Chmelka, B. F., Gatenholm, P., & Nordstierna, L. (2016). 13C NMR assignments of regenerated cellulose from solid-state 2D NMR spectroscopy. *Carbohydrate Polymers, 151*, 480–487.

Isogai, A., & Kato, Y. (1998). Preparation of polyuronic acid from cellulose by tempo-mediated oxidation. *Cellulose, 5*, 153–164.

Jesus, P. C. C., Pellosi, D. S., & Tedesco, A. C. (2019). Magnetic nanoparticles: Applications in biomedical processes as synergic drug-delivery systems. *Materials for Biomedical Engineering,* 371–396.

Jiang, H., Wu, Y., Han, B., & Zhang, Y. (2017). Effect of oxidation time on the properties of cellulose nanocrystals from hybrid poplar residues using the ammonium persulfate. *Carbohydrate Polymers, 174*, 291–298.

Keshk, S., & Sameshima, K. (2006). Influence of lignosulfonate on crystal structure and productivity of bacterial cellulose in a static culture. *Enzyme and Microbial Technology, 40*, 4–8.

Klemm, D., Philipp, B., Heinze, T., Heinze, U., & Wagenknecht, W. (1998). *Comprehensive cellulose chemistry; fundamentals and analytical methods.* Weinheim: Wiley-VCH 251p.

Kronenthal, R. L. (1975). Biodegradable polymers in medicine and surgery. *Polymers Medicine and Surgery,* 119–137.

Lemke, C. H., Dong, R. Y., Michal, C. A., & Hamad, W. Y. (2012). New insights into nanocrystalline cellulose structure and morphology based on solid-state NMR. *Cellulose, 19*, 1619–1629.

Li, H., Wu, B., Mu, C., & Lin, W. (2011). Concomitant degradation in periodate oxidation of carboxymethyl cellulose. *Carbohydrate Polymers, 84*, 881–886.

Li, J., Wan, Y., Li, L. F., Liang, H., & Wang, J. (2009). Preparation and characterization of 2,3-dialdehyde bacterial cellulose for potential biodegradable tissue engineering scaffolds. *Material Science Engineering. 29*, 1635–1642.

Luz, E. P. C. G., Borges, M. F., Andrade, F. K., Rosa, M. F., Infantes-Molina, A., Rodriguez-Castellón, E., et al. (2018). Strontium delivery systems based on bacterial cellulose and hydroxyapatite for guided bone regeneration. *Cellulose, 25*, 6661–6679.

Mohite, B. V., & Patil, S. V. (2014). A novel biomaterial: Bacterial cellulose and its new era applications. *Biotechnology Applied Biochemical, 61*, 101–110.

Niamsap, T., Lam, N. T., & Sukyai, P. (2019). Production of hydroxyapatite-bacterial nanocellulose scaffold with assist of cellulose nanocrystals. *Carbohydrate Polymers, 205*, 159–166.

Rajwade, J. M., Paknikar, K. M., & Kumbhar, J. V. (2015). Applications of bacterial cellulose and its composites in biomedicine. *Applied Microbiology and Biotechnology, 99*, 2491–2511.

Ribeiro, M., Moraes, M. A., Beppu, M. M., Garcia, M. P., Fernandes, M. H., Monteiro, F. J., et al. (2015). Development of silk fibroin/nanohydroxyapatite composite hydrogels for bone tissue engineering. *European Polymer Journal, 67*, 66–77.

Saska, S., Barud, H. S., Gaspar, A. M. M., Marchetto, R., Ribeiro, S. J. L., & Messaddeq, Y. (2011). Bacterial cellulose-hydroxyapatite nanocomposites for bone regeneration. *International Journal of Biomaterials, 2011*, 1–8.

Segal, L., Creely, J. J., Martin, A. E., & Conrad, C. M. (1959). An empirical method for estimating the degree of crystallinity of native cellulose using the x-ray diffractometer. *Textile Research Journal, 29*, 786–794.

Seo, B. K., Ryu, H. K., Park, Y. C., Huh, J. E., & Baek, Y. H. (2016). Dual effect of WIN-34B on osteogenesis and osteoclastogenesis in cytokine-induced mesenchymal stem cells and bone marrow cells. *Journal of Ethnopharmacology, 193*, 227–236.

Siller, M., Amer, H., Bacher, M., Roggenstein, W., Rosenau, T., & Potthast, A. (2015). Effects of periodate oxidation on cellulose polymorphs. *Cellulose, 22*, 2245–2261.

Sun, B., Hou, Q., Liu, Z., & Ni, Y. (2015). Sodium periodate oxidation of cellulose nanocrystal and its application as a paper wet strength additive. *Cellulose, 22*, 1135–1146.

Tanskul, S., Amornthatree, K., & Jaturonlak, N. (2013). A new cellulose-producing bacterium, Rhodococcus sp. MI 2: Screening and optimization of culture conditions. *Carbohydrate Polymers, 92*, 421–428.

Topalovic, T., Nierstrasz, V. A., Bautista, L., Jocic, D., Navarro, A., & Warmieskerken, M. M. C. G. (2007). XPS and contact angle study of cotton surface oxidation by catalytic bleaching. *Colloids and Surfaces A: Physicochemical and Engineering Aspects, 296*, 76–85.

Yang, M., Zhen, W., Che, H., & Shan, Z. (2016). Biomimetic design of oxidized bacterial cellulose-gelatin-hydroxyapatite nanocomposites. *Journal of Bionic Engineering, 13*, 631–640.